

# **SANDIA REPORT**

SAND2013-3714

Unlimited Release

Printed May and 2013

## **Measurements of Prompt Radiation Induced Conductivity in Teflon (PTFE)**

E.F Hartman, T. A. Zarick, T. J. Sheridan, E. F. Preston

Prepared by  
Sandia National Laboratories  
Albuquerque, New Mexico 87185 and Livermore, California 94550

Sandia National Laboratories is a multi-program laboratory managed and operated by Sandia Corporation, a wholly owned subsidiary of Lockheed Martin Corporation, for the U.S. Department of Energy's National Nuclear Security Administration under contract DE-AC04-94AL85000.

Approved for public release; further dissemination unlimited.



**Sandia National Laboratories**

Issued by Sandia National Laboratories, operated for the United States Department of Energy by Sandia Corporation.

**NOTICE:** This report was prepared as an account of work sponsored by an agency of the United States Government. Neither the United States Government, nor any agency thereof, nor any of their employees, nor any of their contractors, subcontractors, or their employees, make any warranty, express or implied, or assume any legal liability or responsibility for the accuracy, completeness, or usefulness of any information, apparatus, product, or process disclosed, or represent that its use would not infringe privately owned rights. Reference herein to any specific commercial product, process, or service by trade name, trademark, manufacturer, or otherwise, does not necessarily constitute or imply its endorsement, recommendation, or favoring by the United States Government, any agency thereof, or any of their contractors or subcontractors. The views and opinions expressed herein do not necessarily state or reflect those of the United States Government, any agency thereof, or any of their contractors.

Printed in the United States of America. This report has been reproduced directly from the best available copy.

Available to DOE and DOE contractors from

U.S. Department of Energy  
Office of Scientific and Technical Information  
P.O. Box 62  
Oak Ridge, TN 37831

Telephone: (865) 576-8401  
Facsimile: (865) 576-5728  
E-Mail: [reports@adonis.osti.gov](mailto:reports@adonis.osti.gov)  
Online ordering: <http://www.osti.gov/bridge>

Available to the public from

U.S. Department of Commerce  
National Technical Information Service  
5285 Port Royal Rd.  
Springfield, VA 22161

Telephone: (800) 553-6847  
Facsimile: (703) 605-6900  
E-Mail: [orders@ntis.fedworld.gov](mailto:orders@ntis.fedworld.gov)  
Online order: <http://www.ntis.gov/help/ordermethods.asp?loc=7-4-0#online>



SAND2013-3714  
Unlimited Release  
Printed May 2013

# Measurements of Prompt Radiation Induced Conductivity in Teflon (PTFE)

E.F Hartman, T. A. Zarick, T. J. Sheridan  
Radiation Effects Experimentation  
Sandia National Laboratories  
P.O. Box 5800  
Albuquerque, New Mexico 87185-MS1167

E. Preston  
ITT Exelis Mission Systems  
655 Space Center Drive  
Colorado Springs, CO 80915-3604

## Abstract

We performed measurements of the prompt radiation induced conductivity (RIC) in thin samples of Teflon (PTFE) at the Little Mountain Medusa LINAC facility in Ogden, UT. Three mil (76.2 microns) samples were irradiated with a 0.5  $\mu$ s pulse of 20 MeV electrons, yielding dose rates of 1E9 to 1E11 rad/s. We applied variable potentials up to 2 kV across the samples and measured the prompt conduction current. Details of the experimental apparatus and analysis are reported in this report on prompt RIC in Teflon.

## **ACKNOWLEDGMENTS**

The authors acknowledge the excellent support of the Boeing employees at the Little Mountain LINAC Facility near Ogden, UT. The editing support of Diana Wrobel was appreciated in the preparation of this report.

# CONTENTS

1.	Introduction .....	7
2.	Test Summary.....	7
3.	Experimental Apparatus and Test Chamber.....	8
4.	TFE1 .....	12
5.	TFE2.....	14
6.	TFE3b.....	16
7.	Summary .....	17
8.	Bibliography.....	19
9.	Distribution.....	21

# FIGURES

Figure 1	A RIC cell test fixture.	8
Figure 2	A typical RIC cell.	9
Figure 3	The vacuum experimental chamber.	10
Figure 4	The experiment chamber with high voltage cables.	10
Figure 5	Typical unbiased (a) and biased (b) waveforms from the TFE1 series.	12
Figure 6	The RIC coefficient fit for the TFE1 URC.	13
Figure 7	Unbiased, low biased, and high biased waveforms from the TFE2 series.	14
Figure 8	RIC coefficient fit for the TFE2 URC.	15
Figure 9	Typical unbiased and biased shots from the TFE3b series.	16
Figure 10	RIC coefficient fit for the TFE3b URC.	16
Figure 11	Conductivity vs. dose rate, and the fit.	18

# TABLES

Table 1	Test Summary	7
Table 2	Fits for the RIC Coefficient and Conductivity	17



## 1. INTRODUCTION

We performed measurements of the prompt radiation induced conductivity (RIC) in thin samples of Teflon (PTFE) at the Little Mountain Medusa LINAC facility in Ogden, UT. Three mil (76.2 microns) samples were irradiated with a 0.5  $\mu$ s pulse of 20 MeV electrons, yielding dose rates of 1E9 to 1E11 rad/s. We applied variable potentials up to 2 kV across the samples and measured the prompt conduction current. Details of the experimental apparatus and analysis are reported in this report on prompt RIC in Teflon.

## 2. TEST SUMMARY

Three different Teflon RIC cells were used, each containing an upper RIC cell (URC) and a lower RIC cell (LRC). The sample number is labeled as TFEX, where X is 1-3. The specific test series is labeled as indicated in the table below.

**Table 1 Test Summary**

Date	Sample / Series	TLD type	Shot Numbers	Nominal Dose Rate (rad/s)	Nominal Pulse Width (ns)
June 2005	TFE1	LiF	1211-1257	3.5E10	500
July 2007	TFE3a-1	Si	1061-1077	2.2E9	500
	TFE3a-2	Si	1078-1094	4.1E9	500
	TFE3a-3	SI	1095-1107	8.4E9	500
	TFE2-1	Si	1237-1249	2.5E9	500
	TFE2-2	Si	1250-1262	4.4E9	500
	TFE2-3	SI	1263-1275	8.5E9	500
December 2008	TFE3b	SI	2247-2307	1.1E11	35

The ratios between the dose in the Teflon layers and the measured dose in the TLD's, as computed by MCNP, is 1.05 (URC) and 1.04 (LRC) for the LiF TLD, and 0.99 (URC) and 1.00 (LRC) for the Si Calorimeter. All dose rates reported are scaled to the dose in Teflon.

### 3. EXPERIMENTAL APPARATUS AND TEST CHAMBER

Figure 1 shows a side view cross-section of the RIC test fixture for the dielectric samples. This configuration is a stack of two separate cells which are irradiated together. Each cell consists of a center electrode, two dielectric layers, and ground planes on the outer surface of each dielectric. The RIC cell nearest the electron beam is called the upper RIC cell (URC), and the cell below it the lower RIC cell (LRC).

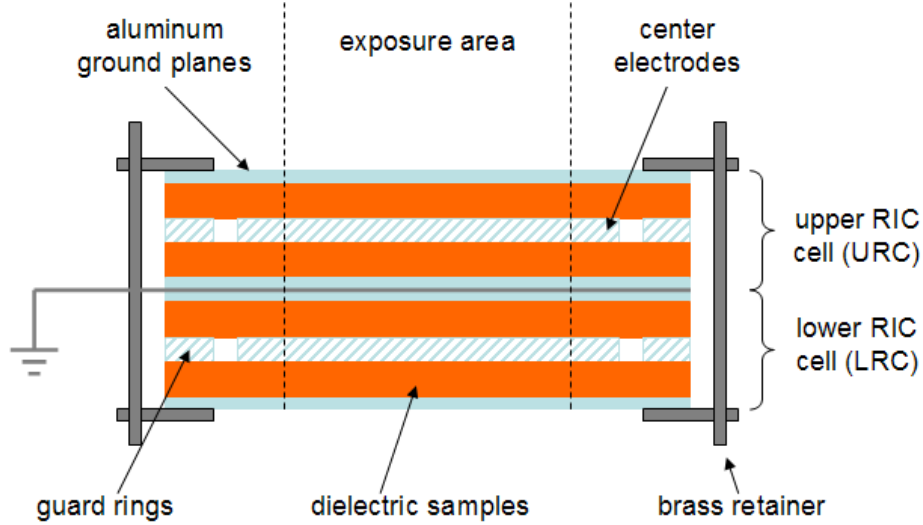


Figure 1 A RIC cell test fixture.

The Teflon layers are formed from 76.2 micron thick discs, about 2.5 centimeters in diameter, and are placed on either side of a 30 micron center aluminum electrode. Two 15 micron outer aluminum electrodes serve as the cell ground planes. The guard rings minimize the electric field distortion at the edge of the center electrodes. Bias voltages were applied to the center electrodes and the guard rings. The bias of the lower cell was made equal to that of the upper cell, with opposite polarity.

Current is driven through the dielectric layers from their conductivity and the applied bias, and directly from the attenuation and divergence of the electron beam. The conductivity consists of the dark or static conductivity  $\sigma_0$ , the prompt RIC  $\sigma_p$ , and the delayed RIC  $\sigma_d$ . The net current is the sum

$$I = Vd(\sigma_0 + \sigma_p + \sigma_d) + I_{dd} \quad (1)$$

where  $V$  is the bias, and  $d$  the sample thickness. The delayed conductivity may contain several terms with different decay constants, representing traps of different depths. In addition, there is a direct drive current  $I_{dd}$  produced by the electron beam in the absence of bias.

This cell design, including dielectric layers above and below a center electrode, greatly reduces the direct drive current,  $I_{dd}$  by balancing the charge lost from the center electrode on either side.

Even with this technique, the direct drive current is a substantial part of the total, and it can be difficult to determine the contribution of the prompt RIC for polymers.

A typical RIC cell test fixture is pictured in Figure 2. The busses for applying the guard ring voltages (LGR and UGR) and the center electrode biases (URC and LRC) are labeled.

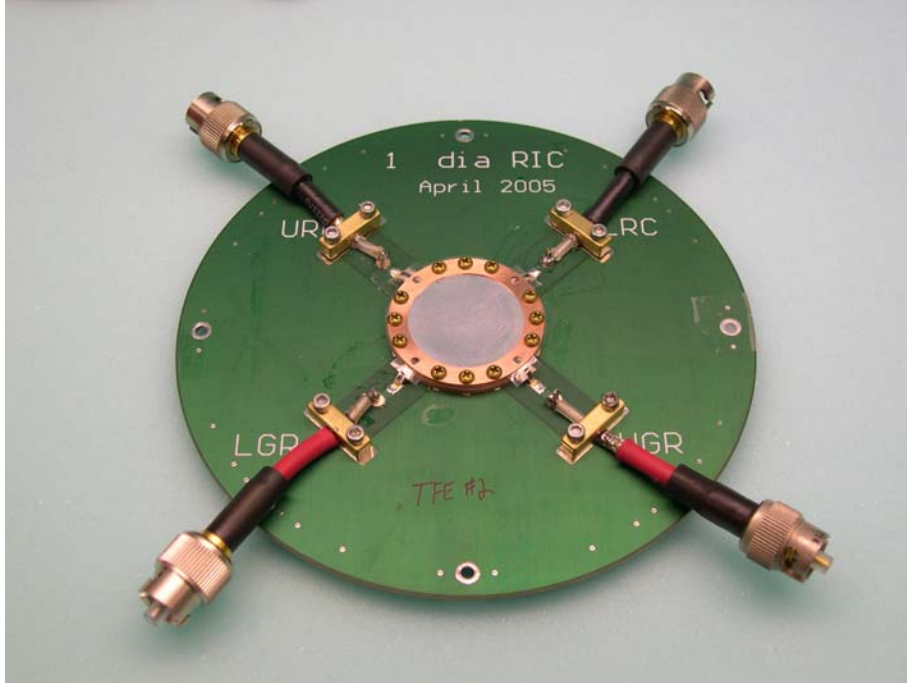


**Figure 2 A typical RIC cell.**

The properties of the Teflon samples under test are given below.

**Composition** (weight fractions): C 0.240183, F 0.759818

**Density:** 2.25 g/cm<sup>3</sup>

**Dielectric constant:** 2.02

**Sample thickness:** 3.00 mils = 76.2 microns

The measured capacitance of the RIC cells containing Teflon is 2.48E+02 pf with a standard deviation of 6.05pf. This is for one two- sided cell, either the URC or the LRC. The area of the center electrode is  $A_{tot} = 5.06 \text{ cm}^2$ , but the irradiated area was collimated to  $1.98 \text{ cm}^2$ . The measured capacitance closely agrees with a one-dimensional calculation:

$$C = \frac{2A_{tot}k\epsilon_0}{d} = \frac{2(5.06 \times 10^{-4} \text{ m}^2)(2.02)(8.9 \times 10^{-12} \text{ F / m})}{76.2 \times 10^{-6} \text{ m}} = 239 \text{ pF} . \quad (2)$$

The test chamber that housed the RIC (radiation induced conductivity) cell was evacuated to  $2E-4$  Torr to eliminate any effects due to air ionization. Radiation entered the test chamber through a collimated aperture. Figure 3 shows the front side of the test chamber and the aperture hole in the center of the fixture. The aperture was smaller in diameter than the dielectric samples, assuring that only the central area of the dielectric was struck by radiation, and that the guard rings did not receive radiation exposure. Figure 4 shows the side view of the test chamber with the front of the LINAC visible to the right.

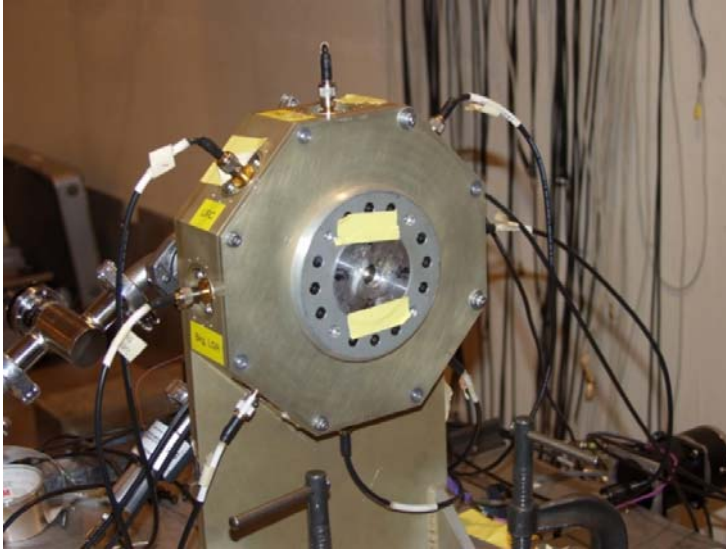


**Figure 3 The vacuum experimental chamber. It shown in the foreground with high voltage cables exiting through vacuum feed-through connectors.**

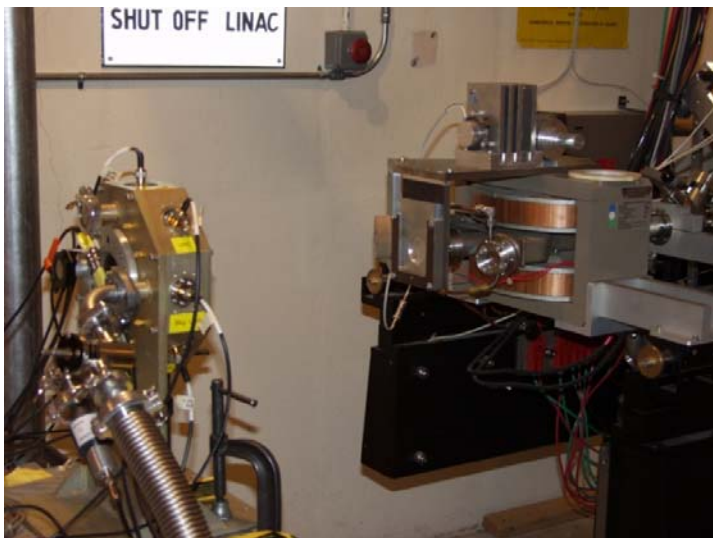


**Figure 4 The experiment chamber with high voltage cables. In the background is the front of the Little Mountain Medusa LINAC facility.**

### **Electron Beam Characteristics**

If a radiation source is not capable of providing consistent or repeatable output, including its spectrum, pulse width, and fluence, then the difficulty of performing repeatable and interpretable experiments is greatly magnified. We chose the Medusa LINAC at the Little Mountain Test Facility (LMTF) because it is capable of producing repeatable and predictable radiation output over long periods of time (such as reproducible pulsing over a week of experiments). We found through repeated testing that our dosimetry consisting of silicon calorimeter, PIN diode and PCD diamond detectors gave consistent repeatable readings shot to shot for the same conditions such as fixed distance from the source and fixed pulse width. The variation at the same conditions was approximately 1% shot to shot.

The nominal electron energy for the LINAC is 20 MeV, and the radiation pulse can be varied from 10 ns to 50  $\mu$ s. For most of these experiments the radiation pulse width was about 0.5  $\mu$ s FWHM. The dose rate range for this experiment was about 1E9 to 1E10 rad(Si)/s. For electron beam dosimetry, silicon calorimeters were supplemented with TLDs, PIN diodes, and PCDs. Measurement accuracy at the LINAC, including dosimetry and recording instruments, is estimated to be about  $\pm 10\%$ .

## 4. TFE1

Typical waveforms for the TFE1 series are shown in figure 5. The direct drive signal is about 0.2 to 0.3 Volts and the biased signal (at 400 V) is about 0.4 V, so the RIC current is producing about a 0.1 V difference. The positively biased cell has its signal reduced from the 0.2 V present from the direct drive to about 0.1 V, as expected. You can see the delayed RIC driving a slight negative voltage in the positively biased cell after the pulse, when the direct drive contribution is removed.

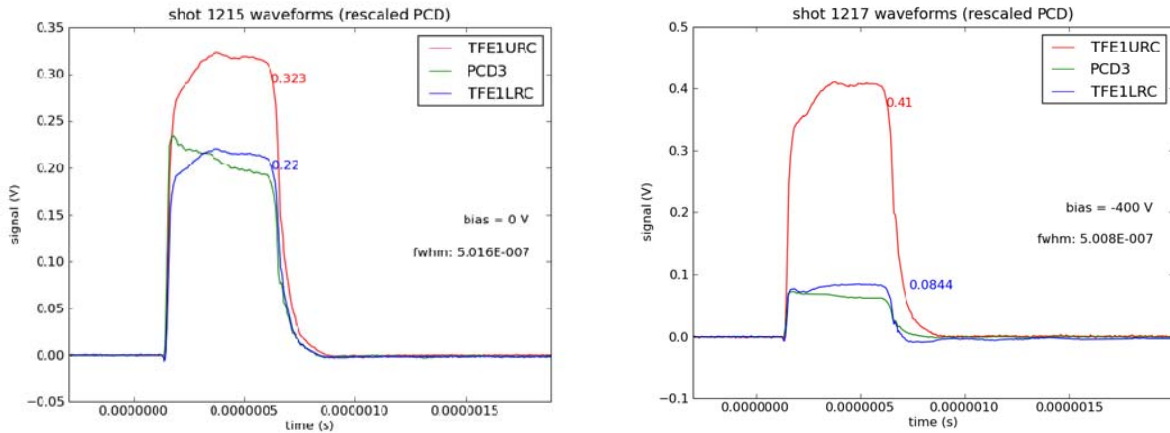


**Figure 5 Typical unbiased (a) and biased (b) waveforms from the TFE1 series.**

The URC data for the TFE1 series is shown in figure 6. There is a problem with the data for positive bias above 800 V, so these are excluded from the fit. A few other outlying points were also excluded. The mean dose rate was used. Unlike other material samples (like Pyralux), there is no change in slope or intercept going from negative to positive bias.

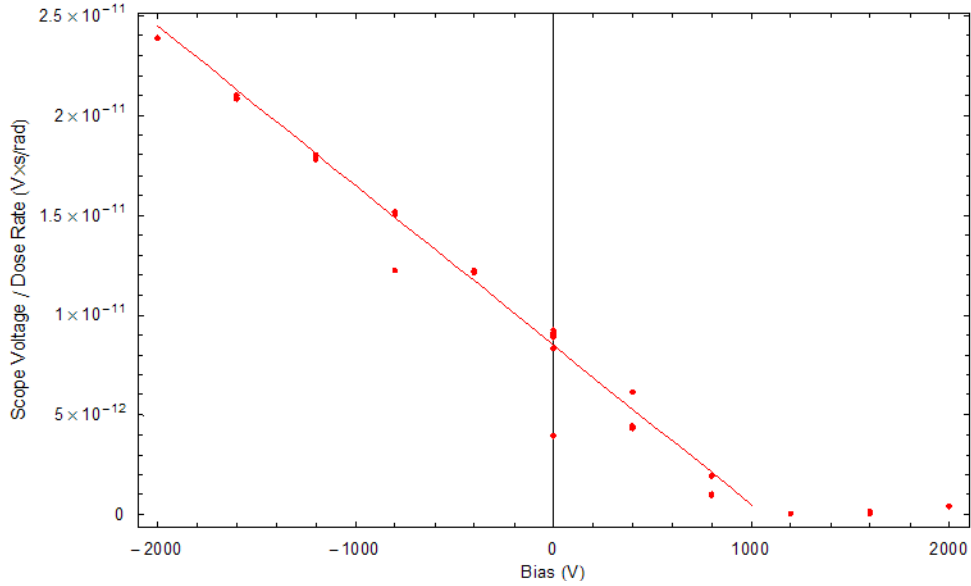


**Figure 6 The RIC coefficient fit for the TFE1 URC.**

## 5. TFE2

The TFE 2 cells had highly asymmetric responses as seen in figure 7. The URC direct drive response is about half the LRC direct drive response. At low bias, there is the expected asymmetry in the signals due to direct drive, but at high bias, the positively biased cell shows a larger response.

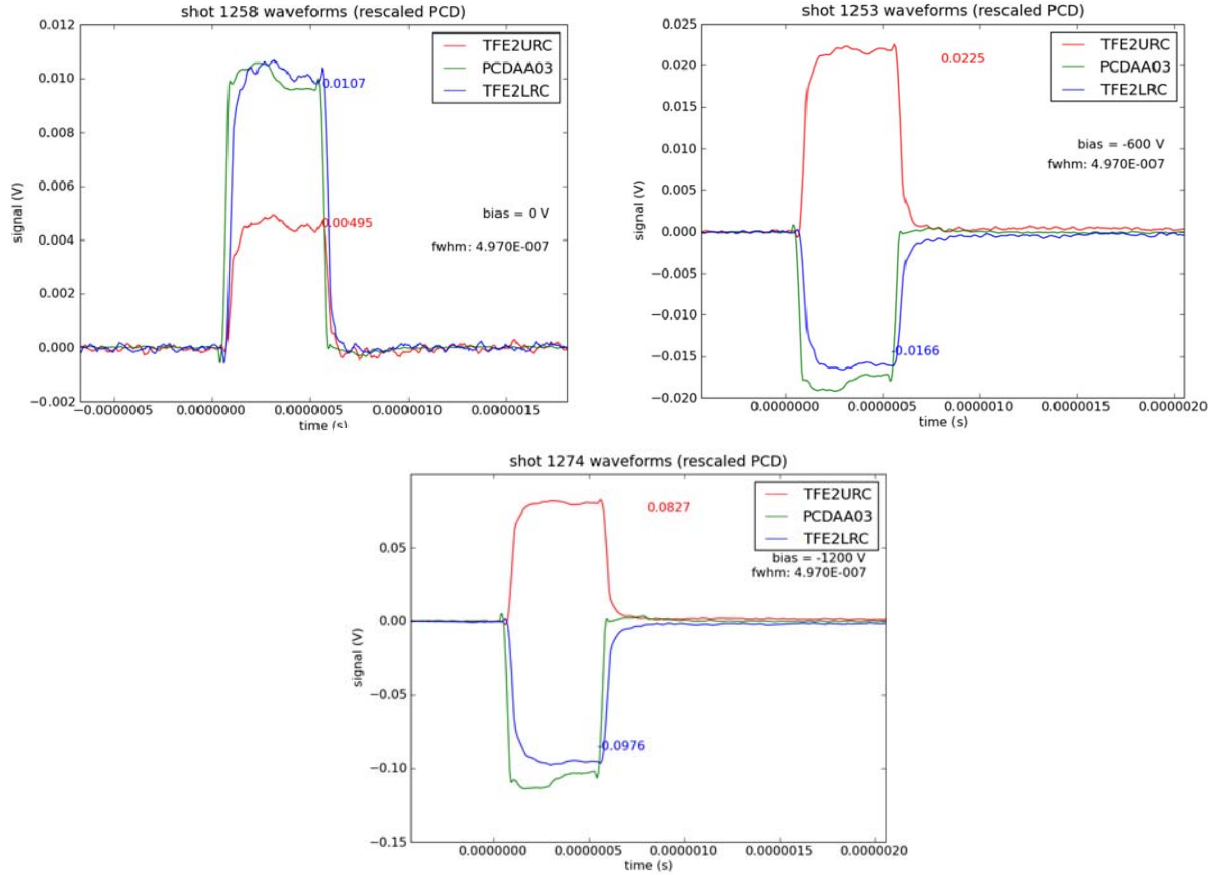
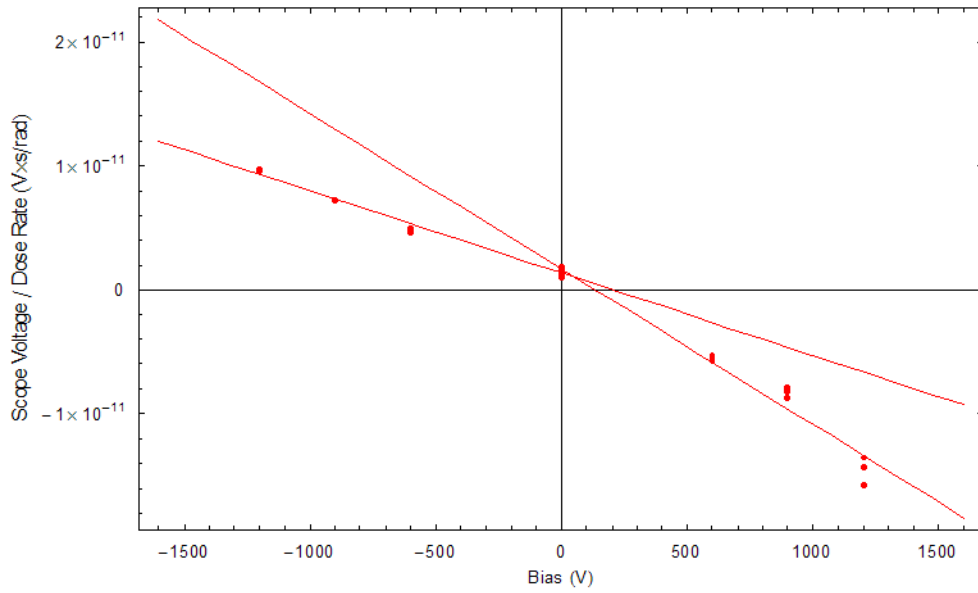


Figure 7 Unbiased, low biased, and high biased waveforms from the TFE2 series.

The resulting RIC coefficient fit (figure8) shows a small discontinuity at zero, but a larger slope for positive bias. This behavior has been observed for most other materials we studied. For consistency, the negative bias data are again used to determine the RIC coefficient.



**Figure 8 RIC coefficient fit for the TFE2 URC.**

## 6. TFE3B

This series was performed with a narrow pulse width around 35 ns. Typical waveforms from this series are shown in figure 9.

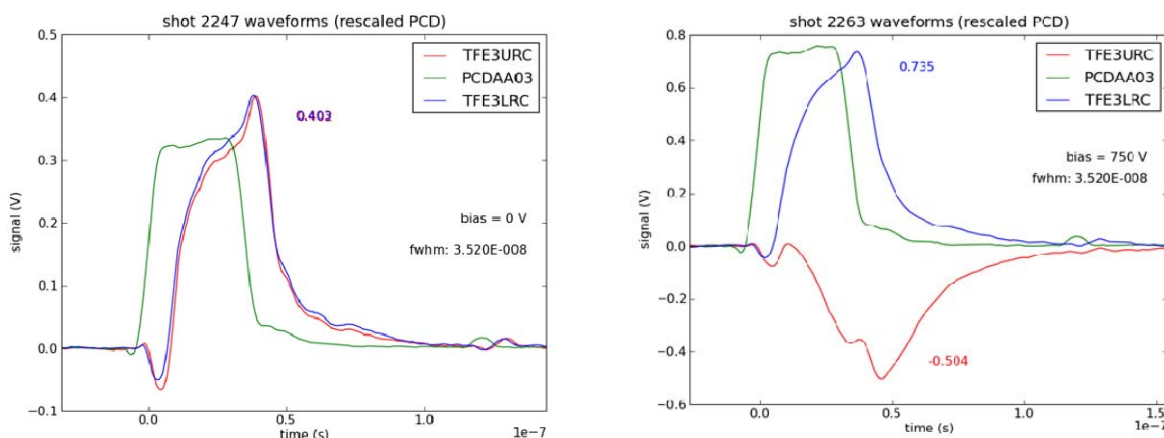


**Figure 9 Typical unbiased and biased shots from the TFE3b series.**

In these narrow pulses, neither the direct drive nor the RIC current reach equilibrium during the pulse, as can be seen from the ramping behavior. The interpretation of these signal features is discussed in the report on RIC in Pyralux. In order to avoid measuring just the delayed RIC, the values for the fit are taken at the time determined by 90% FWHM into the pulse. The RIC coefficient fit is shown in Figure 10.

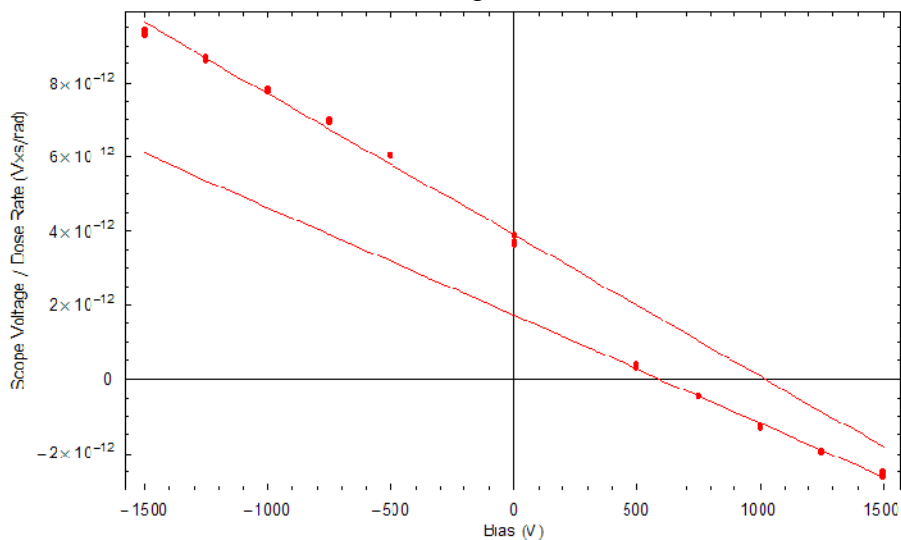


**Figure 10 RIC coefficient fit for the TFE3b URC.**

The shallower slope for positive bias is a feature not seen in any other series. As usual, the negative bias fit is used to determine the RIC coefficient. The measured conductivity is less than would be predicted at this dose rate from the other data, but this is expected due to the narrow pulse width.

## 7. SUMMARY

The resulting fits for the RIC coefficient and conductivity are summarized in the table below. The parentheses indicate the standard error in the slope fit in the last digit.

**Table 2 Fits for the RIC Coefficient and Conductivity**

Series	Cell	Dose rate (rad/s)	k (Mho/m/(rad/s))	$\sigma$ (Mho/m)
TFE1	URC	3.5E10	3.1(1)E-17	1.23(4)E-6
TFE1	LRC	3.5E10	2.75(6)E-17	9.6(2)E-7
TFE3a-1	URC	2.2E9	3.0(1)E-17	6.5(2)E-8
TFE3a-1	LRC	2.2E9	3.1(1)E-17	6.7(2)E-8
TFE3a-2	URC	4.1E9	2.96(6)E-17	1.21(2)E-7
TFE3a-2	LRC	4.1E9	2.90(5)E-17	1.20(2)E-7
TFE3a-3	URC	8.4E9	3.30(6)E-17	2.78(5)E-7
TFE3a-3	LRC	8.5E9	3.22(4)E-17	2.73(4)E-7
TFE2-1	URC	2.5E9	2.6(1)E-17	6.3(4)E-8
TFE2-1	LRC	2.4E9	2.3(1)E-17	5.7(3)E-8
TFE2-2	URC	4.4E9	2.6(1)E-17	1.17(6)E-7
TFE2-2	LRC	4.4E9	2.4(1)E-17	1.08(5)E-7
TFE2-3	URC	8.5E9	3.07(5)E-17	2.60(4)E-7
TFE2-3	LRC	8.5E9	2.87(7)E-17	2.44(6)E-7
TFE3b	URC	1.086(5)E11	1.73(3)E-17	1.87(7)E-6
TFE3b	LRC	1.086(5)E11	1.73(6)E-17	1.87(7)E-6

The conductivities are plotted versus dose rate in figure 11.

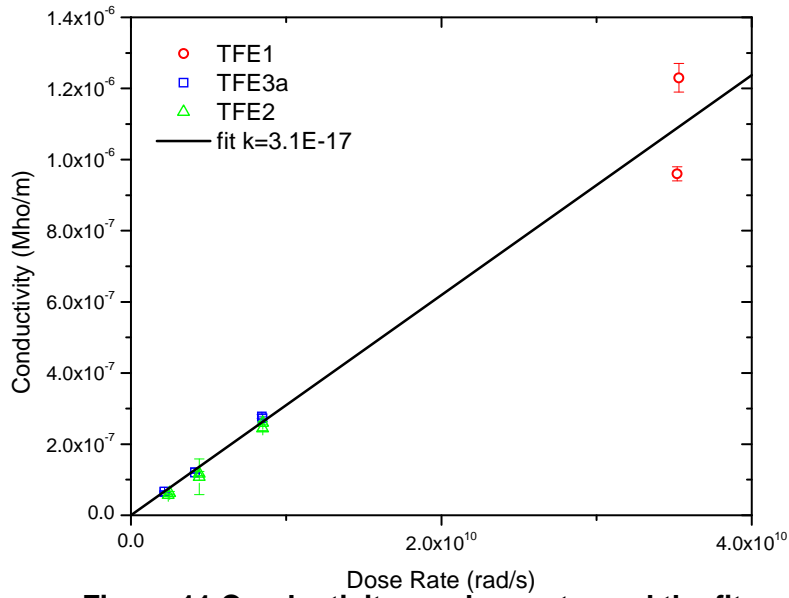


**Figure 11 Conductivity vs. dose rate, and the fit.**

The best fit is purely linear, with a RIC coefficient of  $3.1 \times 10^{-17}$  Mho/m/(rad/s).

## 8. BIBLIOGRAPHY

1. E.F. Hartman, T. A. Zarick, T. J Sheridan, E.F. Preston, T. A. Stringer  
“Measurement of Prompt Radiation Induced Conductivity of Kapton”,  
SAND2010-7284, October 2010
2. Thomas J. Ahrenst and Frederick Wooten, "Electrical Conductivity Induced in Insulators by Pulsed Radiation," Nuclear Science, IEEE Transactions on, vol. 23, pp. 1268-1272, 1976.
3. D. K. Nichols and V. A. J., "Theory of Transient Electrical Effects in Irradiated Insulators," Nuclear Science, IEEE Transactions on, vol. 13, pp. 119-126, 1966.
4. L. Weaver, J. Kenneth Shultis, and R. E. Faw, "Analytic solutions of a model for radiation-induced conductivity in insulators," Journal of Applied Physics, vol. 48, pp. 2762-2770, 1977.
5. J. F. Fowler, "X-Ray Induced Conductivity in Insulating Materials," Proceedings of the Royal Society of London A, vol. 236, pp. 464-480, 1956.
6. J. Mort and D. M. Pai, Eds., Photoconductivity and Related Phenomena.: Elsevier, 1976.
7. E. F. Hartman, "Measurements of Prompt Radiation Induced Conductivity of Fiberglass," Sandia National Laboratories Report SAND2010-2080 Sandia National Laboratories, 2010.
8. V. J. Harper-Slaboszewicz, "Dosimetry Experiments at the Medusa Facility (Little Mountain)," Sandia National Laboratories Report SAND2010-6771 Sandia National Laboratories, 2010.
9. E.J. Yadlowsky and R.C. Hazelton, "Radiation induced conduction in Kapton H film," Nuclear Science, IEEE Transactions on, vol. 35, pp. 1050-1054, 1988.
10. R.H.; Hofer W.;; "Measurements of X-Ray-Induced Photoconductivity and Charge Transfers in Dielectric Structures," IEEE Trans. Nucl. Sci. Vol. NS-19, vol. 6, 1973.
11. J. Frenkel, "On Pre-Breakdown Phenomena in Insulators and Electronic Semi-Conductors," Phys. Rev., vol. 54, pp. 647-648, 1938.
12. H. Frohlich, "On the Theory of Dielectric Breakdown in Solids," Proceedings of the Royal Society of London. Series A. Mathematical and Physical Sciences, vol. 188, pp. 521-532, 1947.
13. H Fröhlich and J O'Dwyer, "Time Dependence of Electronic Processes in Dielectrics," Proceedings of the Physical Society. Section A, vol. 63, p. 81, 1950.
14. J H Simpson, "The Time Delay in Conduction and Breakdown Processes in Amorphous Solids," Proceedings of the Physical Society. Section A, vol. 63, p. 86, 1950.
15. Steven H. Face, Charles A. Eklund, and Thomas A. Stringer, "Measurement of Radiation Induced Conductivity for Hardened Cable Dielectric Materials at

- High Fluence," Nuclear Science, IEEE Transactions on, vol. 30, pp. 4450-4456, 1983.
16. R. Gregorio Filho, B. Gross, and R. M. Faria, "Induced Conductivity of Mylar and Kapton Irradiated by X-Rays," Electrical Insulation, IEEE Transactions on, vol. EI-21, pp. 431-436, 1986.
  17. R. C. Weingart, R. H. Barlett, R. S. Lee, and W. Hofer, "X-Ray-Induced Photoconductivity in Dielectric Films," Nuclear Science, IEEE Transactions on, vol. 19, pp. 15-22, 1972.
  18. V. A. J., J. W. Harrity, and T. M. Flanagan, "Scaling Laws for Ionization Effects in Insulators," Nuclear Science, IEEE Transactions on, vol. 15, pp. 194-204, 1968.
  19. Berger and Seltzer, "Tables of Energy Loss and Ranges of Electrons and Positrons," NASA, 1964.
  20. A.R. Frederickson, "Radiation Induced Currents and Conductivity in Dielectrics," IEEE Trans. on Nuc. Sci., vol. #NS-24#, 1977.
  21. A.R. Frederickson, S. Woolf, and J.C. Garth, "Model for space charge evolution and dose in irradiated insulators at high electric fields," Nuclear Science, IEEE Transactions on, vol. 40, pp. 1393-1401, 1993.

## 9. DISTRIBUTION

ITT Exelis Mission Systems

Attn: E. F. Preston

655 Space Center Drive

Colorado Springs, CO 80915-3604

1 MS 1152	M.L. Kiefer	01612
1 MS 1152	M.F. Pasik	01652
1 MS 1152	K. Cartwright	01652
1 MS 1152	C.D. Turner	01652
1 MS 1159	J.W. Bryson	01344
1 MS 1159	K.J. McDonald	01344
5 MS 1167	E.F. Hartman	01343
1 MS 1167	T.A. Zarick	01343
1 MS 1167	T.J. Sheridan	01343
1 MS 1167	T.M. Flanagan	01343
1 MS 1167	M.L. McLain	01343
1 MS 1168	L. X. Scheider	01650
1 MS 1179	L. Lorence	01341
1 MS 1179	C.R. Drumm	01341
1 MS 1179	W. C. Fan	01341
1 MS 1179	H.P. Hjalmarson	01341
1 MS 1159	G.S. Heffelfinger	01340
1 MS 0899	Technical Library	9536 (electronic copy)





**Sandia National Laboratories**